

Astro/Physics 224 Winter 2008

Origin and Evolution of the Universe

Horizons, Big Bang Nucleosynthesis

Lecture 4 - Jan 25, 2008

Joel Primack

University of California, Santa Cruz

EFFECTS OF CURVATURE NEAR A BLACK HOLE

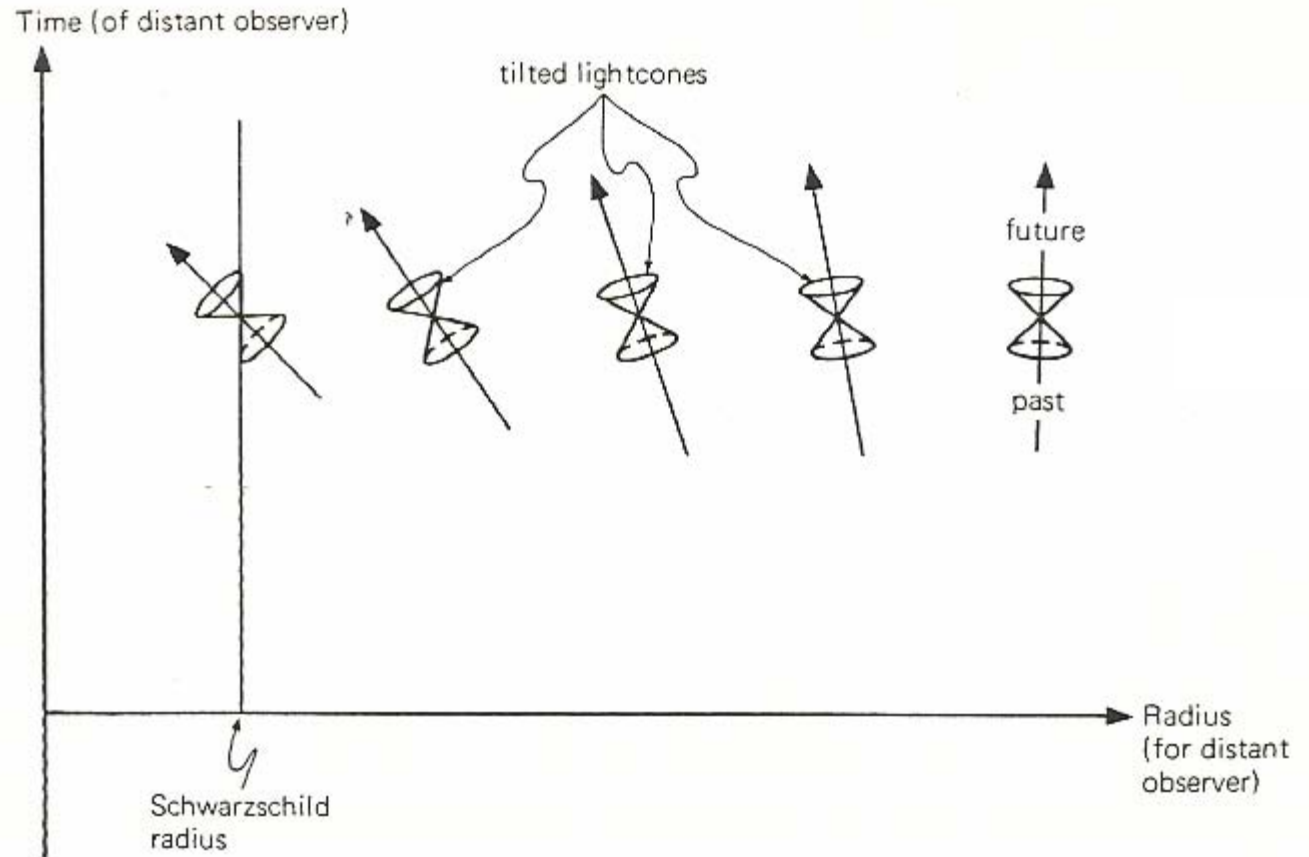
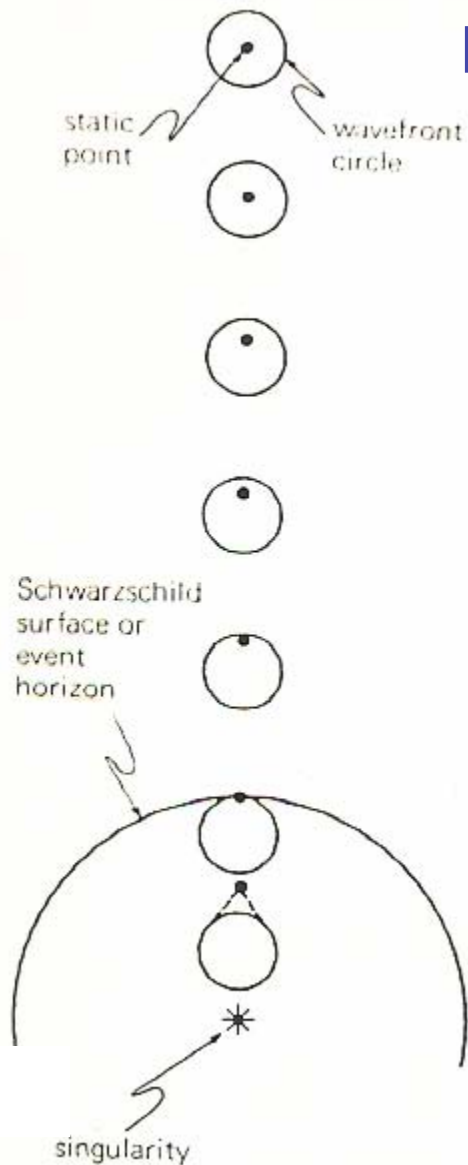


Figure 9.6. The effect of spacetime curvature near a black hole. Lightcones are tilted in such a way that the future-pointing lightcone tips toward the black hole and the past-pointing lightcone tips away from the black hole. At the surface of the black hole (the Schwarzschild surface), all rays emitted in the future direction fall into the black hole, and no rays from the past are received from the black hole. A person passing into a black hole therefore receives no information of what lies ahead.

E. Harrison, Cosmology

LCDM Benchmark Cosmological Model: Ingredients & Epochs

| | List of Ingredients |
|-------------------------------|--|
| photons: | $\Omega_{\gamma,0} = 5.0 \times 10^{-5}$ |
| neutrinos: | $\Omega_{\nu,0} = 3.4 \times 10^{-5}$ |
| total radiation: | $\Omega_{r,0} = 8.4 \times 10^{-5}$ |
| baryonic matter: | $\Omega_{\text{bary},0} = 0.04$ |
| nonbaryonic dark matter: | $\Omega_{\text{dm},0} = 0.26$ |
| total matter: | $\Omega_{m,0} = 0.30$ |
| cosmological constant: | $\Omega_{\Lambda,0} \approx 0.70$ |

| | Important Epochs | |
|----------------------------|-------------------------------|---------------------------------------|
| radiation-matter equality: | $a_{rm} = 2.8 \times 10^{-4}$ | $t_{rm} = 4.7 \times 10^4 \text{ yr}$ |
| matter-lambda equality: | $a_{m\Lambda} = 0.75$ | $t_{m\Lambda} = 9.8 \text{ Gyr}$ |
| Now: | $a_0 = 1$ | $t_0 = 13.5 \text{ Gyr}$ |

Benchmark Model: Scale Factor vs. Time

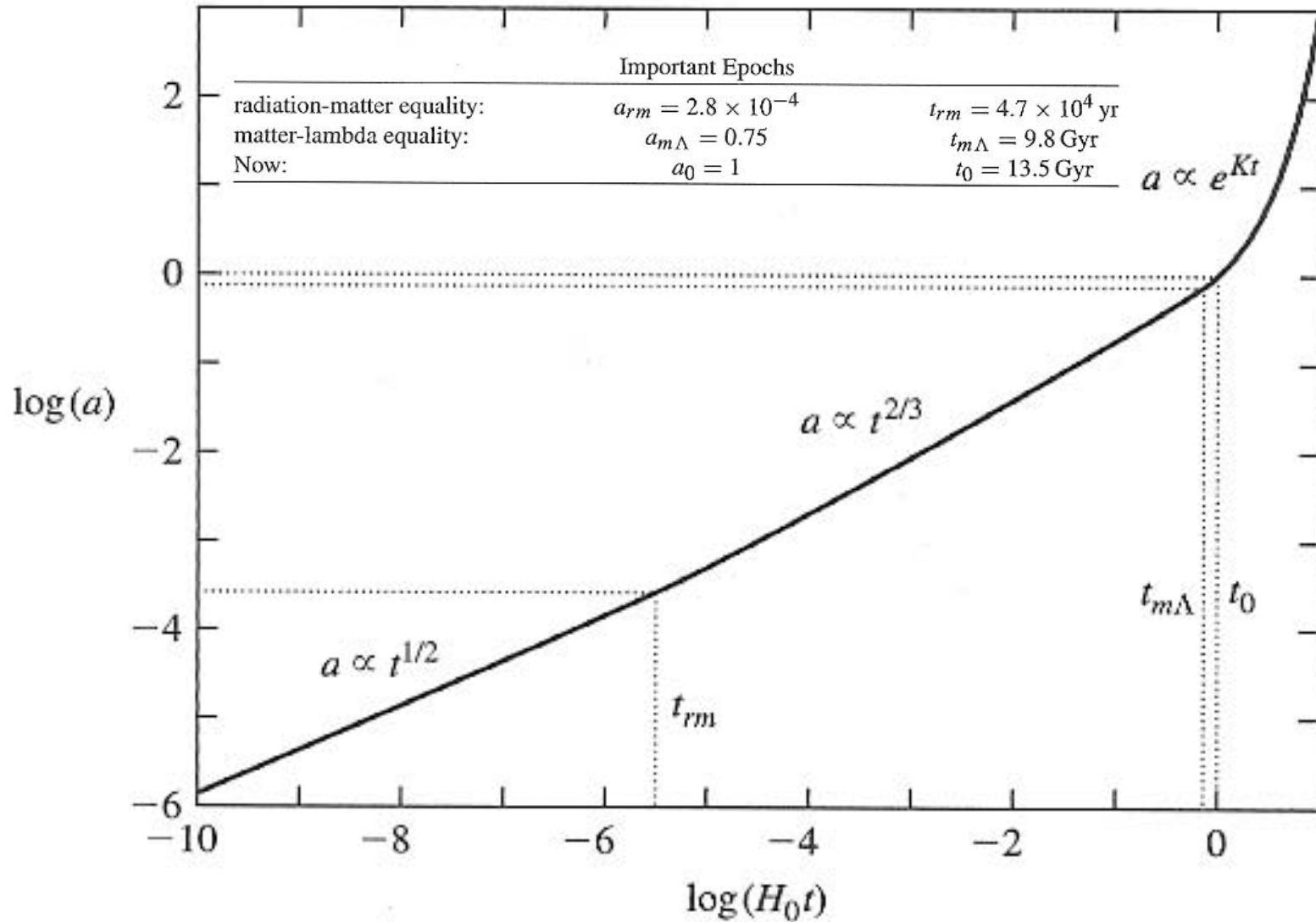
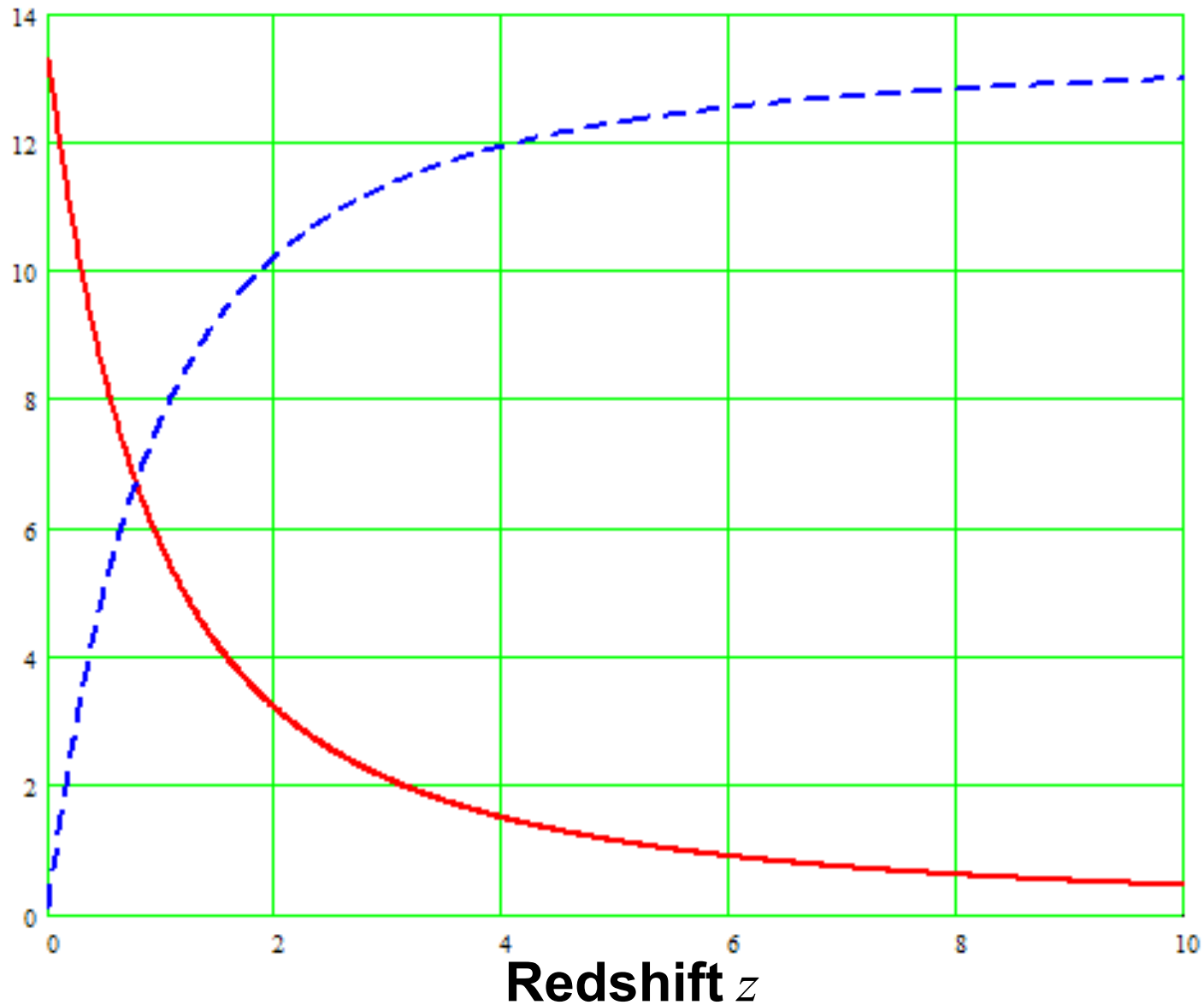


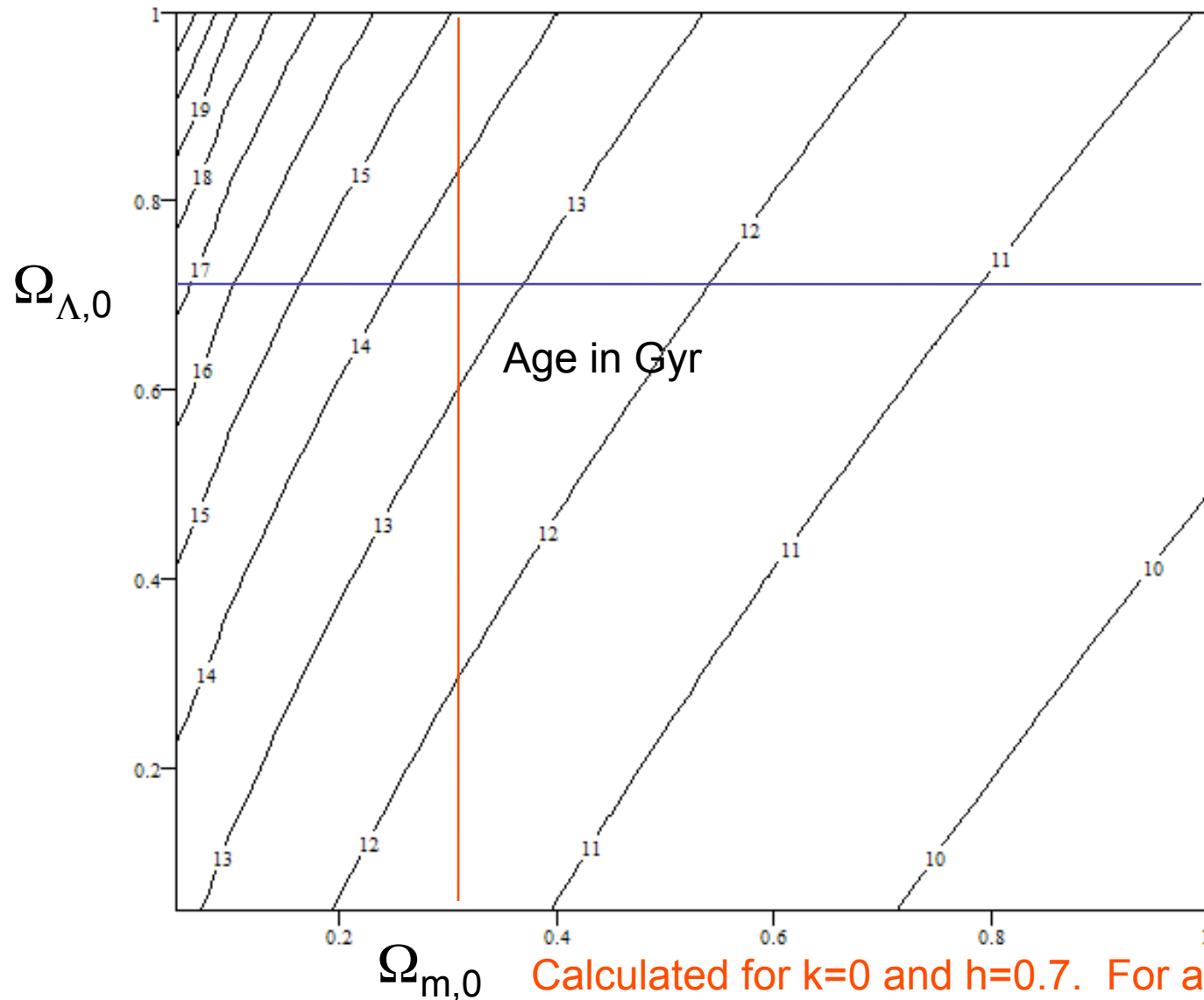
FIGURE 6.5 The scale factor a as a function of time t (measured in units of the Hubble time), computed for the Benchmark Model. The dotted lines indicate the time of radiation-matter equality, $a_{rm} = 2.8 \times 10^{-4}$, the time of matter-lambda equality, $a_{m\Lambda} = 0.75$, and the present moment, $a_0 = 1$.

Age of the Universe and Lookback Time



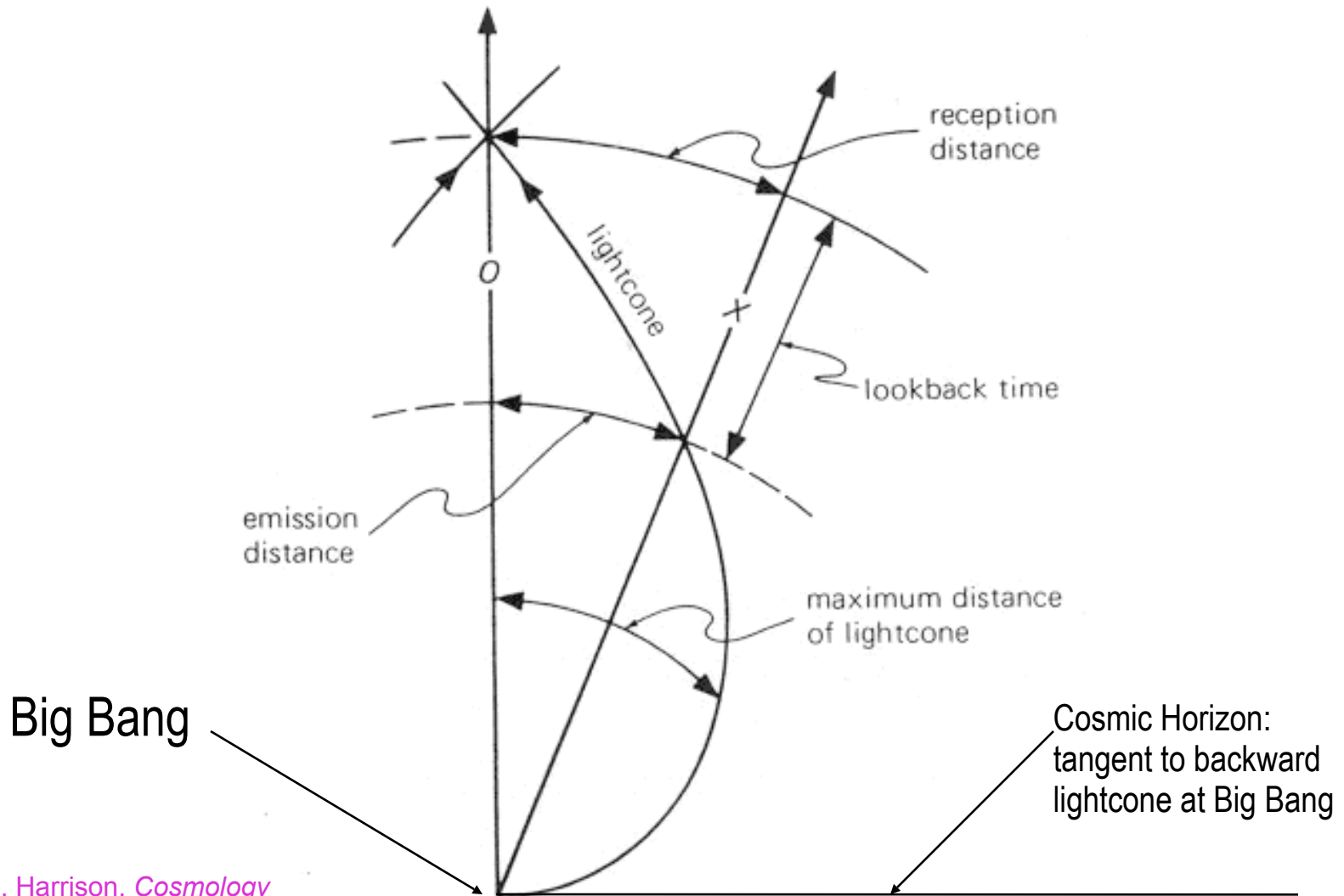
These are for $\Omega_{m,0}=0.3$, $\Omega_{\Lambda,0}=0.7$, $h=0.7$.

Age t_0 of the Double Dark Universe



Calculated for $k=0$ and $h=0.7$. For any other value of the Hubble parameter, multiply the age by $(h/0.7)$.

Picturing the History of the Universe: The Backward Lightcone



From E. Harrison, *Cosmology*
(Cambridge UP, 2000).

Picturing the History of the Universe: The Backward Lightcone

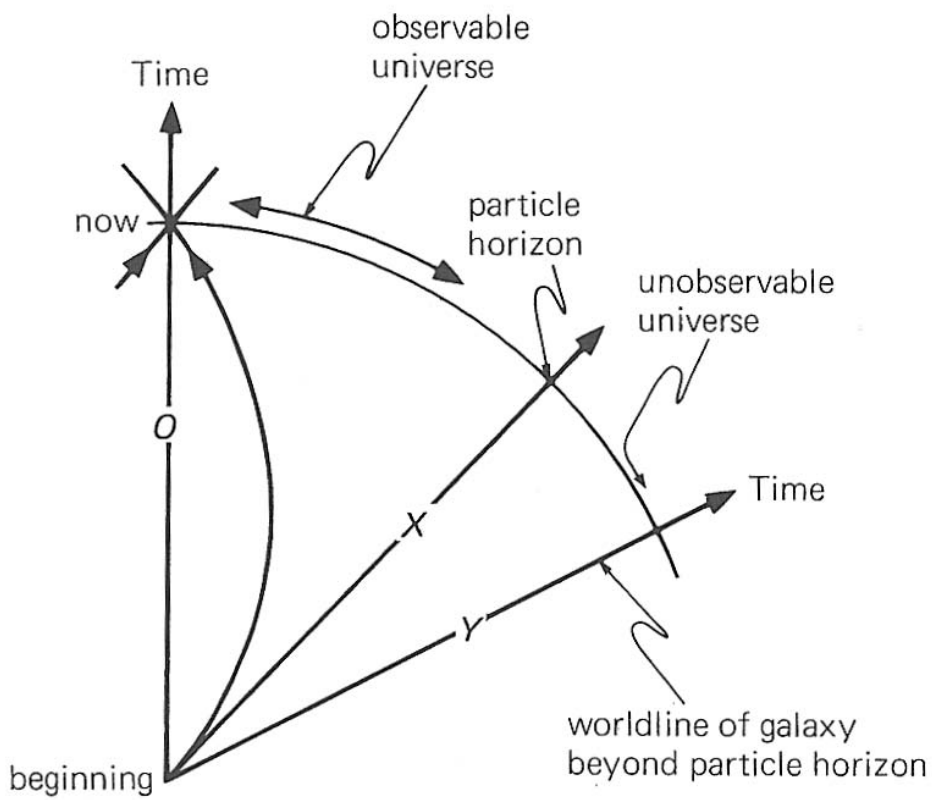


Figure 21.11. At the instant labeled “now” the particle horizon is at worldline X. In a big bang universe, all galaxies at the particle horizon have infinite redshift.

From E. Harrison, *Cosmology* (Cambridge UP, 2000).

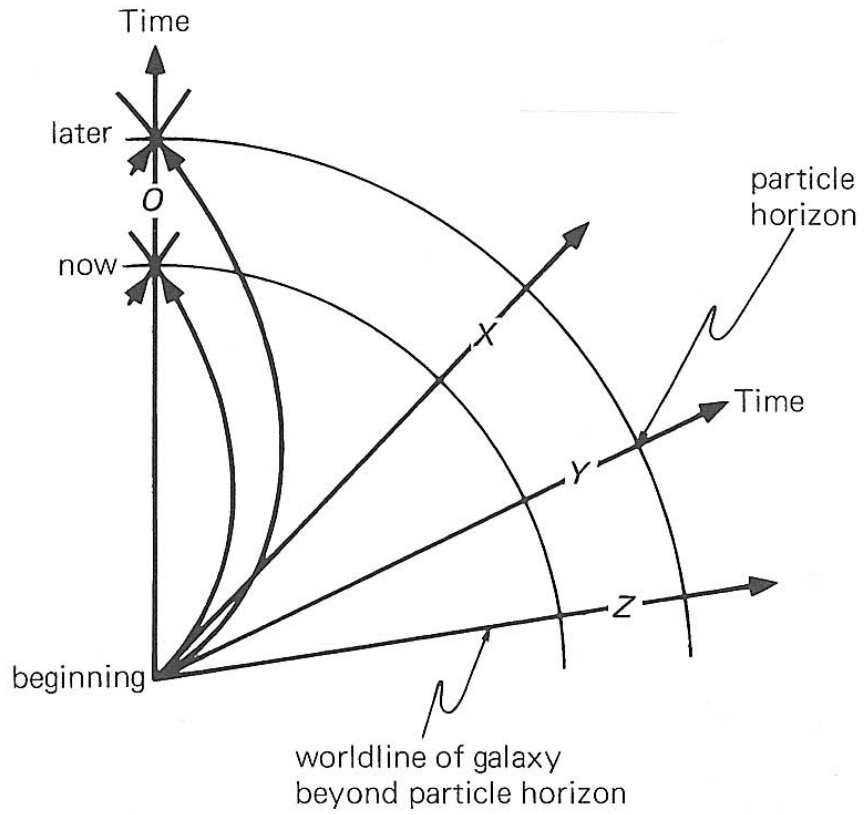


Figure 21.12. At the instant labeled “later” the particle horizon has receded to world line Y. Notice the distance of the particle horizon is always a reception distance, and the particle horizon always overtakes the galaxies and always the fraction of the universe observed increases.

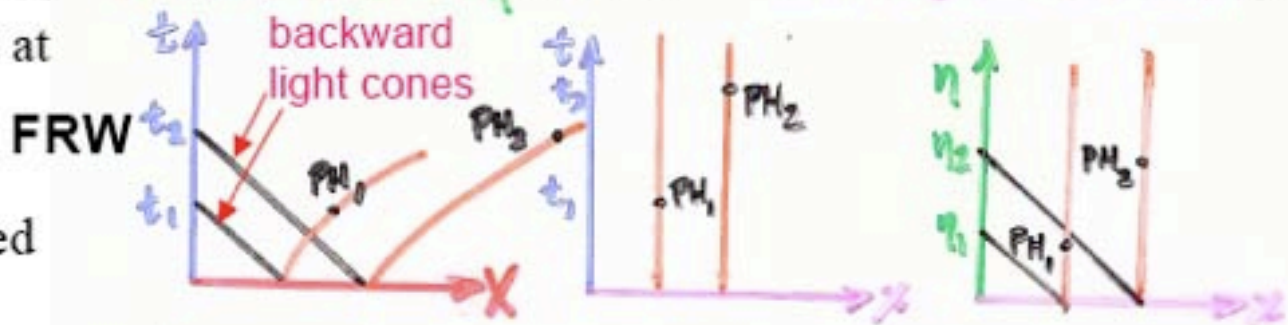
Horizons

PARTICLE HORIZON

Spherical surface that at time t separates *worldlines* into observed vs. unobserved

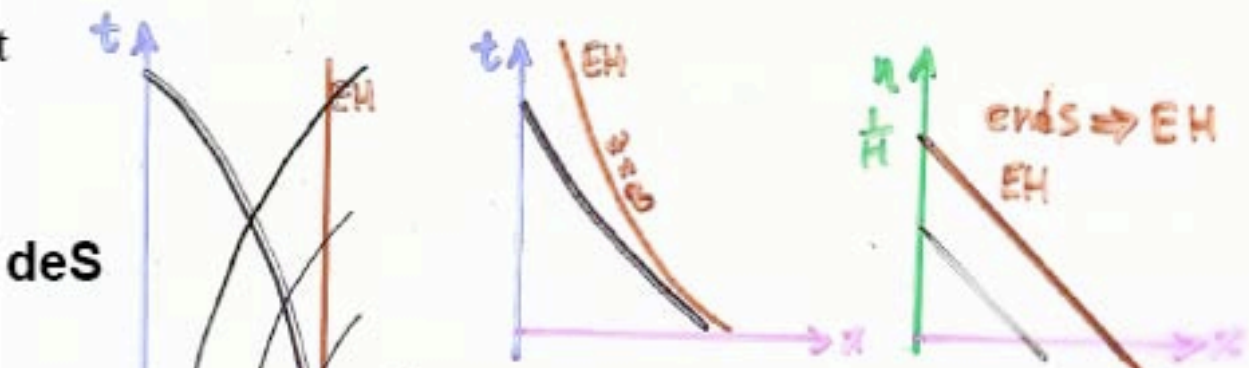
$$ds^2 = dt^2 - dX^2 = dt^2 - R^2 dx^2 = R^2 (d\eta^2 - dx^2)$$

conformal time $d\eta = dt/R$ Comoving coord. $dx = dX/R$



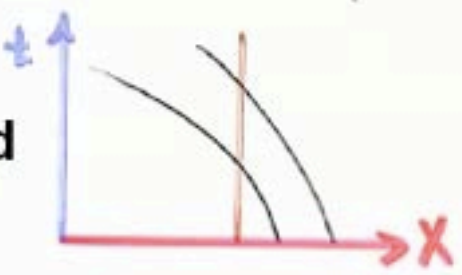
EVENT HORIZON

Backward lightcone that separates *events* that will someday be observed from those never observed



$$\tau = \int_{t_0}^{\infty} \frac{dt}{e^{Ht}} = \frac{1}{H} e^{-Ht_0} \approx \frac{1}{H}$$

Schwarzschild



See Harrison, *Cosmology*
Rindler, *Relativity*

Distances in an Expanding Universe

FRW: $ds^2 = -c^2 dt^2 + a(t)^2 [dr^2 + r^2 d\theta^2 + r^2 \sin^2\theta d\phi^2]$ for curvature $k=0$

$$\chi(t_1) = (\text{comoving distance at time } t_1) = \int_0^{t_1} dt/a = r_1$$

$$d(t_1) = (\text{physical distance at } t_1) = a(t_1) \chi(t_1)$$

Particle $\chi_p = (\text{comoving distance at time } t_0) = r_p$

Horizon $d_p = (\text{physical distance at time } t_0) = a(t_0) r_p = r_p$

since $a(t_0) = 1$

From the FRW metric above, the distance D across a source at distance r_1 which subtends an angle $d\theta$ is $D = a(t_1) r_1 d\theta$. The **angular diameter distance** d_A is defined by $d_A = D/d\theta$, so

$$d_A = a(t_1) r_1 = r_1 / (1+z_1)$$

In Euclidean space, the **luminosity** L of a source at distance d is related to the apparent luminosity ℓ by

$$\ell = \text{Power/Area} = L/4\pi d^2$$

so the **luminosity distance** d_L is defined by $d_L = (L/4\pi\ell)^{1/2}$.

Weinberg, *Gravitation and Cosmology*, pp. 419-421, shows that in FRW

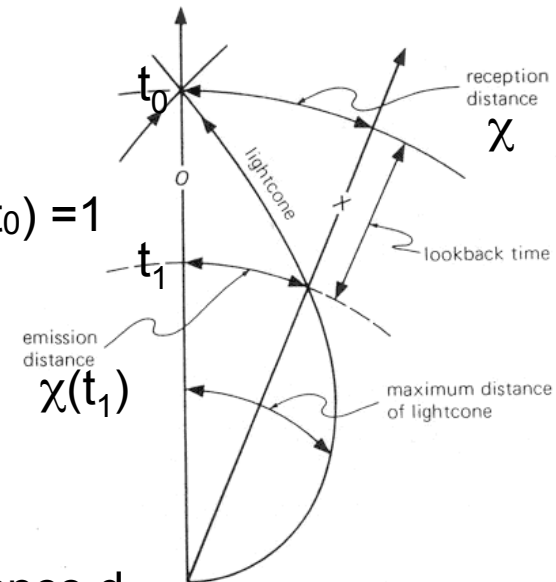
$$\ell = \text{Power/Area} = L [a(t_1)/a(t_0)]^2 [4\pi a(t_0)^2 r_1^2]^{-1} = L/4\pi d_L^2$$

Thus

$$d_L = r_1/a(t_1) = r_1 (1+z_1)$$

fraction of photons reaching unit area at t_0
(redshift of each photon)(delay in arrival)

adding distances at time t_1



Distances in a Flat ($k=0$) Expanding Universe

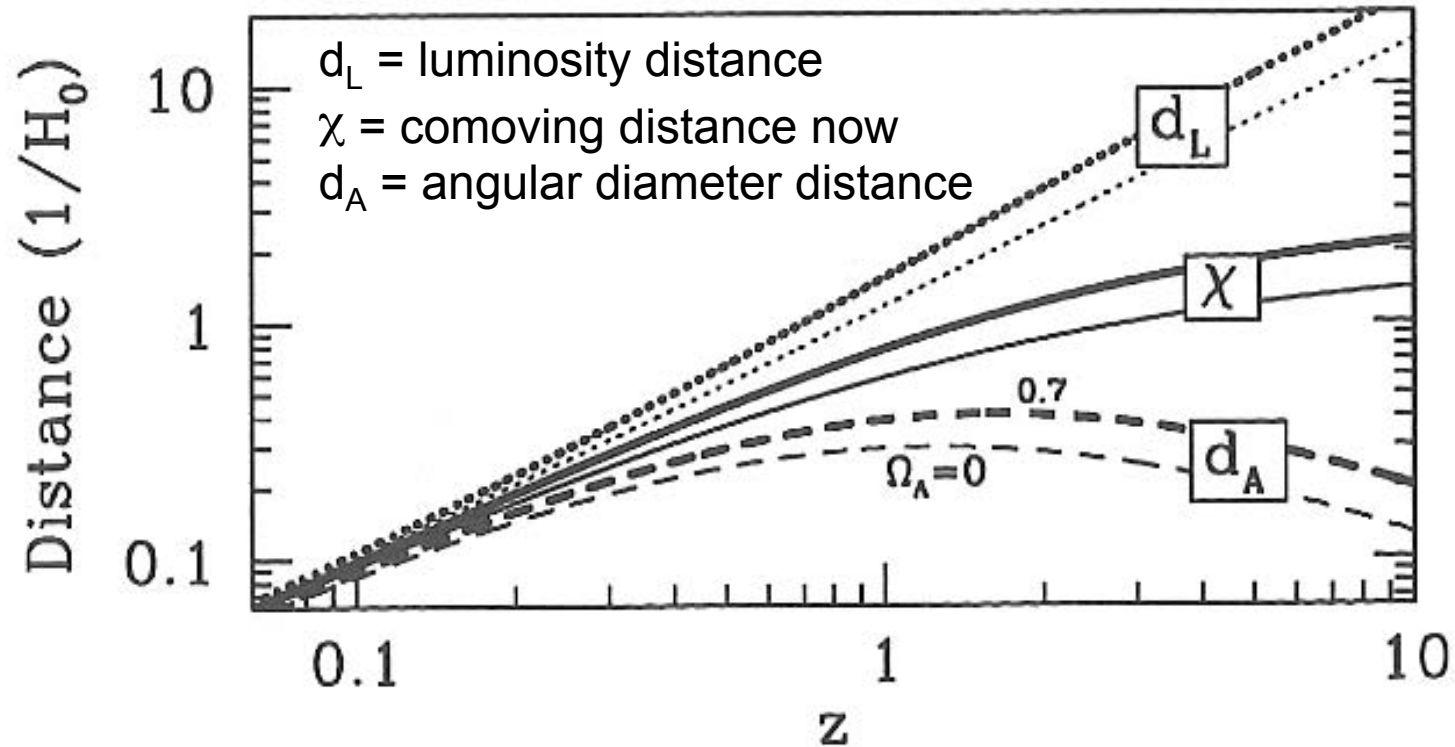


Figure 2.3. Three distance measures in a flat expanding universe. From top to bottom, the luminosity distance, the comoving distance, and the angular diameter distance. The pair of lines in each case is for a flat universe with matter only (light curves) and 70% cosmological constant Λ (heavy curves). In a Λ -dominated universe, distances out to fixed redshift are larger than in a matter-dominated universe.

Neutrino Decoupling and Big Bang Nucleosynthesis, Photon Decoupling, and WIMP Annihilation

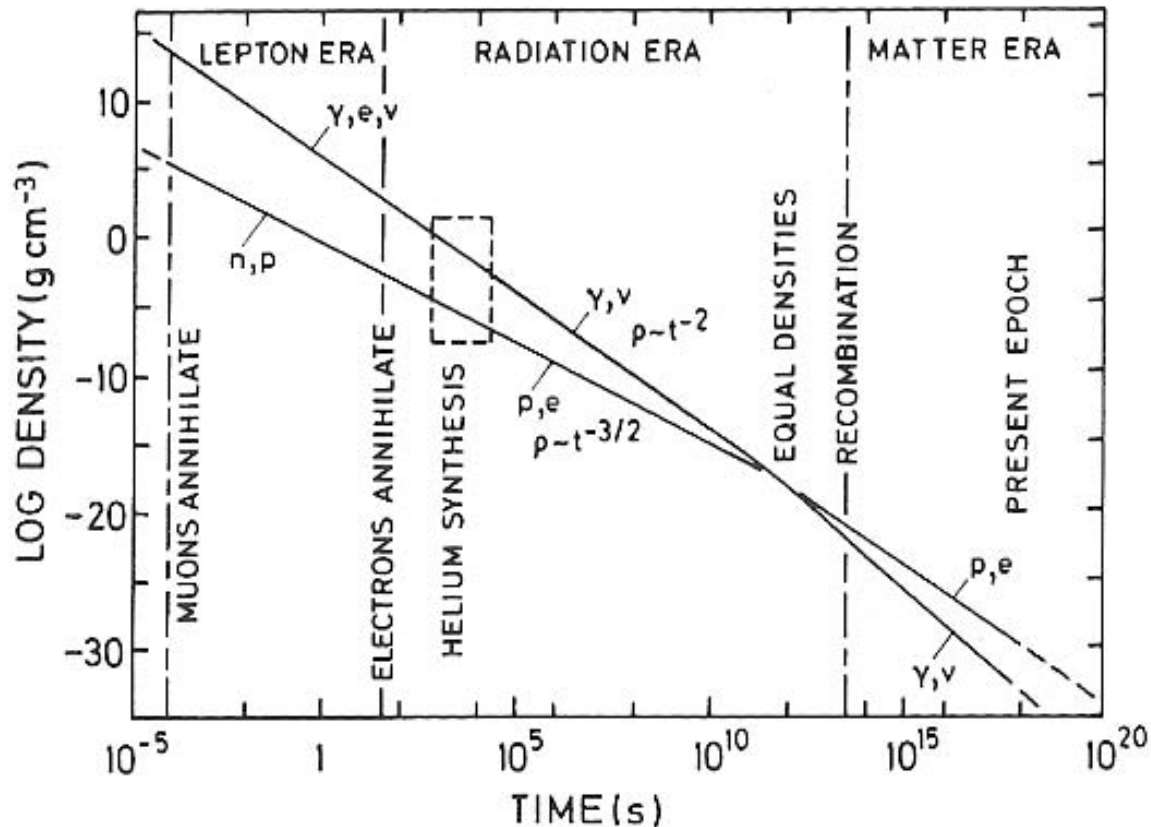
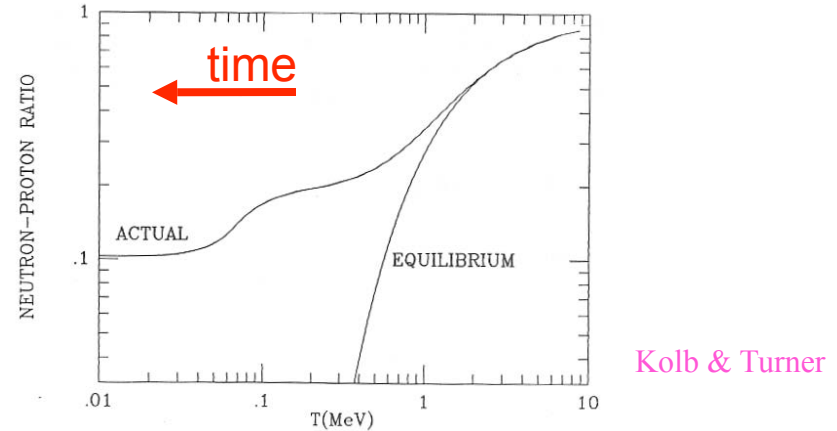
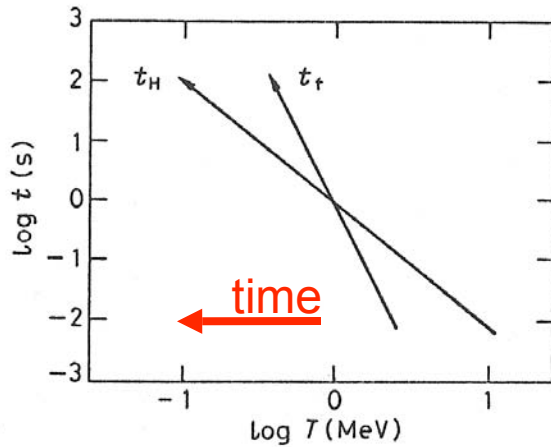


Fig. 3.1. The thermal history of the standard model. The densities of protons, electrons, photons, and neutrinos are shown at various stages of cosmological evolution [after Harrison (1973)]

Big Bang Nucleosynthesis

BBN was conceived by Gamow in 1946 as an explanation for the formation of all the elements, but the absence of any stable nuclei with $A=5,8$ makes it impossible for BBN to proceed past Li. The formation of carbon and heavier elements occurs instead through the triple- α process in the centers of red giants (Burbidge², Fowler, & Hoyle). At the BBN baryon density of $2 \times 10^{-29} \Omega_b h^2 (T/T_0)^3 \text{ g cm}^{-3} \approx 2 \times 10^{-5} \text{ g cm}^{-3}$, the probability of the triple- α process is negligible even though $T \approx 10^9 \text{ K}$.



Thermal equilibrium between n and p is maintained by weak interactions, which keeps $n/p = \exp(-Q/T)$ (where $Q = m_n - m_p = 1.293 \text{ MeV}$) until about $t \approx 1 \text{ s}$. But because the neutrino mean free time $t_\nu^{-1} \approx \sigma_\nu n_{e^\pm} \approx (G_F T)^2 (T^3)$ is increasing as $t_\nu \propto T^{-5}$ (here the Fermi constant $G_F \approx 10^{-5} \text{ GeV}^{-2}$), while the horizon size is increasing only as $t_H \approx (G\rho)^{-1/2} \approx M_{\text{Pl}}^{-1} T^{-2}$, these interactions freeze out when T drops below about 0.8 MeV . This leaves $n/(p+n) \approx 0.14$. The neutrons then decay with a mean lifetime $887 \pm 2 \text{ s}$ until they are mostly fused into D and then ^4He . The higher the baryon density, the higher the final abundance of ^4He and the lower the abundance of D that survives this fusion process. Since D/H is so sensitive to baryon density, David Schramm called deuterium the “baryometer.” He and his colleagues also pointed out that since the horizon size increases more slowly with T^{-1} the larger the number of light neutrino species N_ν contributing to the energy density ρ , BBN predicted that $N_\nu \approx 3$ before N_ν was measured at accelerators by measuring the width of the Z^0 . Latest (Cyburt et al. 2005): $2.67 < N_\nu < 3.85$.

Statistical Thermodynamics

$$n_i = \frac{g_i}{2\pi^2} \left(\frac{kT_i}{hc}\right)^3 I_i''(\pm), \quad \rho_i = \frac{g_i kT_i}{2\pi^2 c^3} \left(\frac{kT_i}{hc}\right)^3 I_i^{2'}(\pm), \quad \text{where}$$

$$I_i^{mn} \equiv \int_{\theta_i}^{\infty} x^m (x^2 - \theta_i^{-2})^{n/2} (e^x \pm 1)^{-1} dx, \quad \theta_i = \frac{kT_i}{m_i c^2}, \quad g_i = \# \text{ spin states}$$

+ Fermi-Dirac, - Bose-Einstein

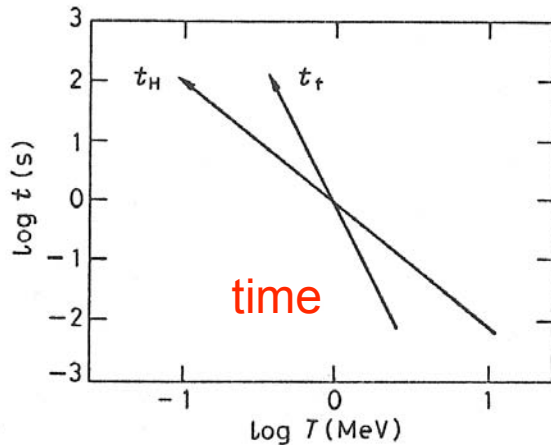
$$\theta_i \gg 1 \quad (\text{ER}): \quad I_i''(+)=\frac{3}{2}\zeta(3)=1.803, \quad I_i^{2'}(+)=7\pi^4/120$$

$$I_i''(-)=2\zeta(3)=\frac{4}{3}I_i''(+), \quad I_i^{2'}(-)=\pi^4/15=\frac{8}{7}I_i^{2'}(+)$$

$$\theta_i \ll 1 \quad (\text{NR}): \quad n_i = \frac{\rho_i}{m_i} = \frac{g_i}{(2\pi)^{3/2}} \left(\frac{kT_i}{hc}\right)^3 \theta_i^{-3/2} e^{-\theta_i^{-1}} \quad (\text{not } \nu's)$$

$$[\text{Note: } \zeta(3) = 1.2020569\dots = \sum_{k=1}^{\infty} \frac{1}{k^3} = \prod_{\text{primes}} (1 - p^{-3})^{-1}]$$

Neutrinos in the Early Universe



As we discussed, neutrino decoupling occurs at $T \sim 1$ MeV. After decoupling, the neutrino phase space distribution is

$$f_\nu = [1 + \exp(p_\nu c / T_\nu)]^{-1} \quad (\text{note: } \neq [1 + \exp(E_\nu / T_\nu)])$$

for NR neutrinos)

After e^+e^- annihilation, $T_\nu = (4/11)^{1/3} T_\gamma = 1.9K$:

Number densities of primordial particles

$$n_\gamma(T) = 2 \zeta(3) \pi^{-2} T^3 = 400 \text{ cm}^{-3} (T/2.7K)^3, \quad n_\nu(T) = \left(\frac{3}{4}\right) n_\gamma(T) \text{ including antineutrinos}$$

FermiDirac/BoseEinstein factor

Conservation of entropy s_i of interacting particles per comoving volume

$s_i = g_i(T) N_\gamma(T) = \text{constant}$, where $N_\gamma = n_\gamma V$; we only include neutrinos for $T > 1$ MeV.

Thus for $T > 1$ MeV, $g_i = 2 + 4(7/8) + 6(7/8) = 43/4$ for γ , e^+e^- , and the three ν species, while for $T < 1$ MeV, $g_i = 2 + 4(7/8) = 11/2$. At e^+e^- annihilation, below about $T = 0.5$ MeV, g_i drops to 2, so that $2N_{\nu 0} = g_i(T < 1 \text{ MeV}) N_\gamma(T < 1 \text{ MeV}) = (11/2) N_\gamma(T < 1 \text{ MeV}) = (11/2)(4/3) N_\nu(T < 1 \text{ MeV})$. Thus $n_{\nu 0} = (3/4)(4/11) n_{\nu 0} = 109 \text{ cm}^{-3} (T/2.7K)^3$, or

$$T_\nu = (4/11)^{1/3} T = 0.714 T$$

Boltzmann Equation

$$a^{-3} \frac{d(n_1 a^3)}{dt} = \int \frac{d^3 p_1}{(2\pi)^3 2E_1} \int \frac{d^3 p_2}{(2\pi)^3 2E_2} \int \frac{d^3 p_3}{(2\pi)^3 2E_3} \int \frac{d^3 p_4}{(2\pi)^3 2E_4} \quad \text{Dodelson (3.1)}$$

In the absence of interactions (rhs=0) n_1 falls as a^{-3}

$$\begin{aligned} & \times (2\pi)^4 \delta^3(p_1 + p_2 - p_3 - p_4) \delta(E_1 + E_2 - E_3 - E_4) |\mathcal{M}|^2 \\ & \times \{f_3 f_4 [1 \pm f_1][1 \pm f_2] - f_1 f_2 [1 \pm f_3][1 \pm f_4]\}. \end{aligned} \quad \begin{array}{l} + \text{ bosons} \\ - \text{ fermions} \end{array}$$

We will typically be interested in $T \gg E - \mu$ (where μ is the chemical potential). In this limit, the exponential in the Fermi-Dirac or Bose-Einstein distributions is much larger than the ± 1 in the denominator, so that

$$f(E) \rightarrow e^{\mu/T} e^{-E/T}$$

and the last line of the Boltzmann equation above simplifies to

$$\begin{aligned} & f_3 f_4 [1 \pm f_1][1 \pm f_2] - f_1 f_2 [1 \pm f_3][1 \pm f_4] \\ & \rightarrow e^{-(E_1 + E_2)/T} \left\{ e^{(\mu_3 + \mu_4)/T} - e^{(\mu_1 + \mu_2)/T} \right\}. \end{aligned}$$

The number densities are given by $n_i = g_i e^{\mu_i/T} \int \frac{d^3 p}{(2\pi)^3} e^{-E_i/T}$. For our applications, i's are

Table 3.1. Reactions in This Chapter: $1 + 2 \leftrightarrow 3 + 4$

| | 1 | 2 | 3 | 4 |
|------------------------|-----|------------------|-----|------------------------|
| Neutron-Proton Ratio | n | ν_e or e^+ | p | e^- or $\bar{\nu}_e$ |
| Recombination | e | p | H | γ |
| Dark Matter Production | X | X | l | l |

$$n_i^{(0)} \equiv g_i \int \frac{d^3 p}{(2\pi)^3} e^{-E_i/T} = \begin{cases} g_i \left(\frac{m_i T}{2\pi}\right)^{3/2} e^{-m_i/T} & m_i \gg T \\ g_i \frac{T^3}{\pi^2} & m_i \ll T \end{cases}. \quad (3.6)$$

With this definition, $e^{\mu_i/T}$ can be rewritten as $n_i/n_i^{(0)}$, so the last line of Eq. (3.1) is equal to

$$e^{-(E_1+E_2)/T} \left\{ \frac{n_3 n_4}{n_3^{(0)} n_4^{(0)}} - \frac{n_1 n_2}{n_1^{(0)} n_2^{(0)}} \right\}. \quad (3.7)$$

With these approximations the Boltzmann equation now simplifies enormously. Define the thermally averaged cross section as

$$\begin{aligned} \langle \sigma v \rangle &\equiv \frac{1}{n_1^{(0)} n_2^{(0)}} \int \frac{d^3 p_1}{(2\pi)^3 2E_1} \int \frac{d^3 p_2}{(2\pi)^3 2E_2} \int \frac{d^3 p_3}{(2\pi)^3 2E_3} \int \frac{d^3 p_4}{(2\pi)^3 2E_4} e^{-(E_1+E_2)/T} \\ &\times (2\pi)^4 \delta^3(p_1 + p_2 - p_3 - p_4) \delta(E_1 + E_2 - E_3 - E_4) |\mathcal{M}|^2. \end{aligned} \quad (3.8)$$

Then, the Boltzmann equation becomes

$$a^{-3} \frac{d(n_1 a^3)}{dt} = n_1^{(0)} n_2^{(0)} \langle \sigma v \rangle \left\{ \frac{n_3 n_4}{n_3^{(0)} n_4^{(0)}} - \frac{n_1 n_2}{n_1^{(0)} n_2^{(0)}} \right\}. \quad (3.9)$$

If the reaction rate $n_2 \langle \sigma v \rangle$ is much smaller than the expansion rate ($\sim H$), then the $\{ \}$ on the rhs must vanish. This is called *chemical equilibrium* in the context of the early universe, *nuclear statistical equilibrium* (NSE) in the context of Big Bang nucleosynthesis, and the *Saha equation* when discussing recombination of electrons and protons to form neutral hydrogen.

As the temperature of the universe cools to 1 MeV, the cosmic plasma consists of:

- **Relativistic particles in equilibrium: photons, electrons and positrons.** These are kept in close contact with each other by electromagnetic interactions such as $e^+e^- \leftrightarrow \gamma\gamma$. Besides a small difference due to fermion/boson statistics, these all have the same abundances.
- **Decoupled relativistic particles: neutrinos.** At temperatures a little above 1 MeV, the rate for processes such as $\nu e \leftrightarrow \nu e$ which keep neutrinos coupled to the rest of the plasma drops beneath the expansion rate. Neutrinos therefore share the same temperature as the other relativistic particles, and hence are roughly as abundant, but they do not couple to them.
- **Nonrelativistic particles: baryons.** If there had been no asymmetry in the initial number of baryons and anti-baryons, then both would be completely depleted by 1 MeV. However, such an asymmetry did exist: $(n_b - n_{\bar{b}})/s \sim 10^{-10}$ initially,¹ and this ratio remains constant throughout the expansion. By the time the temperature is of order 1 MeV, all anti-baryons have annihilated away (Exercise 12) so

$$\eta_b \equiv \frac{n_b}{n_\gamma} = 5.5 \times 10^{-10} \left(\frac{\Omega_b h^2}{0.020} \right). \quad (3.11)$$

There are thus many fewer baryons than relativistic particles when $T \sim \text{MeV}$.

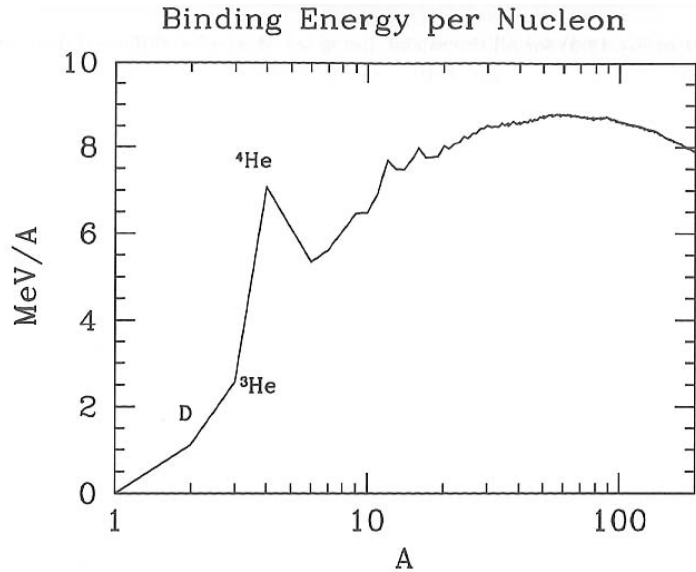


Figure 3.1. Binding energy of nuclei as a function of mass number. Iron has the highest binding energy, but among the light elements, ${}^4\text{He}$ is a crucial local maximum. Nucleosynthesis in the early universe essentially stops at ${}^4\text{He}$ because of the lack of tightly bound isotopes at $A = 5 - 8$. In the high-density environment of stars, three ${}^4\text{He}$ nuclei fuse to form ${}^{12}\text{C}$, but the low baryon number precludes this process in the early universe.

Lightning Introduction to Nuclear Physics

A single proton is a hydrogen nucleus, referred to as ${}^1\text{H}$ or simply p ; a proton and a neutron make up deuterium, ${}^2\text{H}$ or D ; one proton and two neutrons make tritium, ${}^3\text{H}$ or T . Nuclei with two protons are helium; these can have one neutron (${}^3\text{He}$) or two (${}^4\text{He}$). Thus unique elements have a fixed number of protons, and isotopes of a given element have differing numbers of neutrons. The total number of neutrons and protons in the nucleus, the *atomic number*, is a superscript before the name of the element.

The total mass of a nucleus with Z protons and $A - Z$ neutrons differs slightly from the mass of the individual protons and neutrons alone. This difference is called the binding energy, defined as

$$B \equiv Zm_p + (A - Z)m_n - m \quad (3.12)$$

where m is the mass of the nucleus. For example, the mass of deuterium is 1875.62 MeV while the sum of the neutron and proton masses is 1877.84 MeV, so the binding energy of deuterium is 2.22 MeV. Nuclear binding energies are typically in the MeV range, which explains why Big Bang nucleosynthesis occurs at temperatures a bit less than 1 MeV even though nuclear masses are in the GeV range.

Neutrons and protons can interconvert via weak interactions:

$$p + \bar{\nu} \leftrightarrow n + e^+ \quad ; \quad p + e^- \leftrightarrow n + \nu \quad ; \quad n \leftrightarrow p + e^- + \bar{\nu} \quad (3.13)$$

where all the reactions can proceed in either direction. The light elements are built up via electromagnetic interactions. For example, deuterium forms from $p + n \rightarrow \text{D} + \gamma$. Then, $\text{D} + \text{D} \rightarrow n + {}^3\text{He}$, after which ${}^3\text{He} + \text{D} \rightarrow p + {}^4\text{He}$ produces ${}^4\text{He}$.

$$\frac{n_D}{n_n n_p} = \frac{n_D^{(0)}}{n_n^{(0)} n_p^{(0)}}. \quad (3.14)$$

The integrals on the right, as given in Eq. (3.6), lead to

$$\frac{n_D}{n_n n_p} = \frac{3}{4} \left(\frac{2\pi m_D}{m_n m_p T} \right)^{3/2} e^{[m_n + m_p - m_D]/T}, \quad (3.15)$$

the factor of 3/4 being due to the number of spin states (3 for D and 2 each for p and n). In the prefactor, m_D can be set to $2m_n = 2m_p$, but in the exponential the small difference between $m_n + m_p$ and m_D is important: indeed the argument of the

exponential is by definition equal to the binding energy of deuterium, $B_D = 2.22$ MeV. Therefore, as long as equilibrium holds,

$$\frac{n_D}{n_n n_p} = \frac{3}{4} \left(\frac{4\pi}{m_p T} \right)^{3/2} e^{B_D/T}. \quad (3.16)$$

Both the neutron and proton density are proportional to the baryon density, so roughly,

$$\frac{n_D}{n_b} \sim \eta_b \left(\frac{T}{m_p} \right)^{3/2} e^{B_D/T}. \quad (3.17)$$

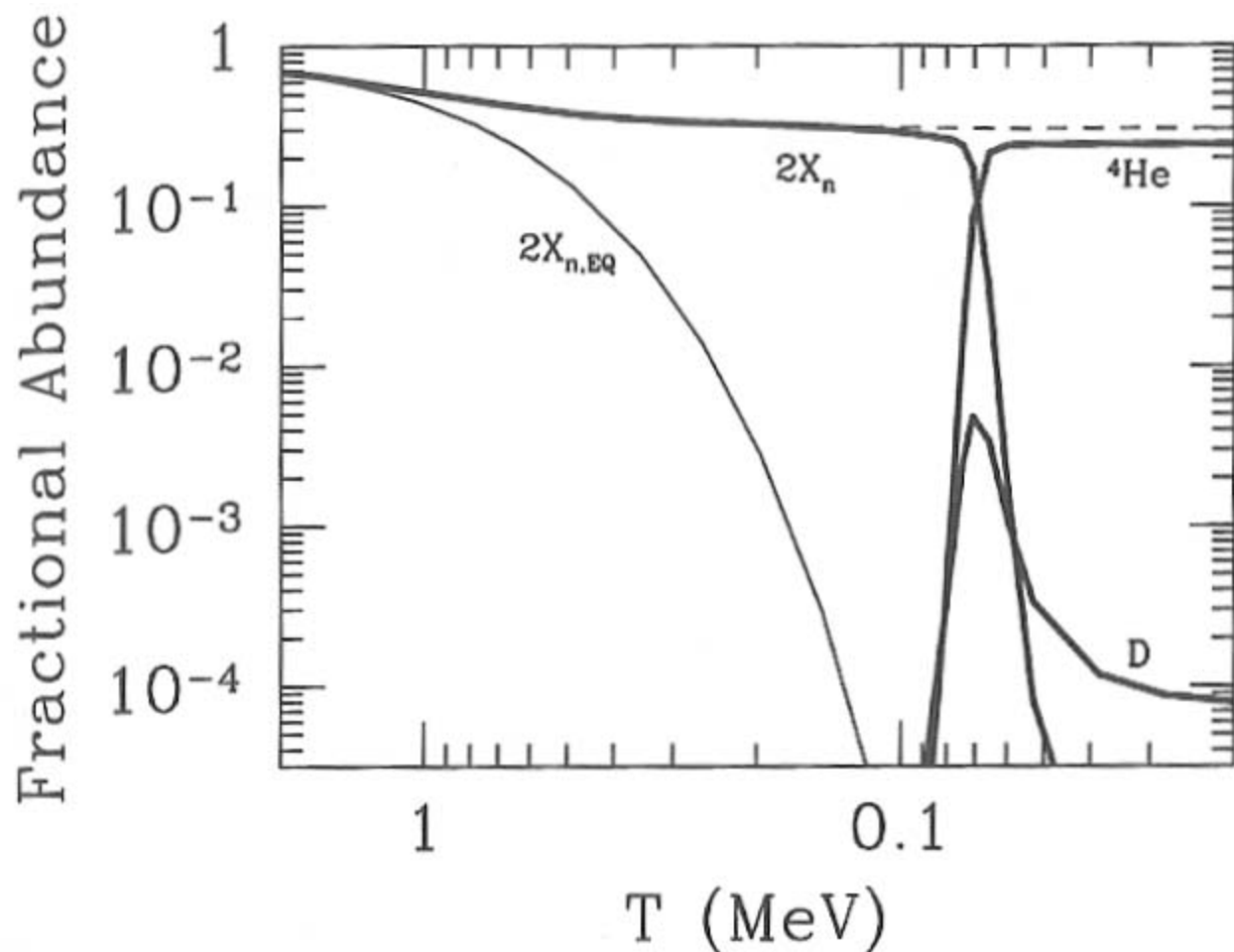
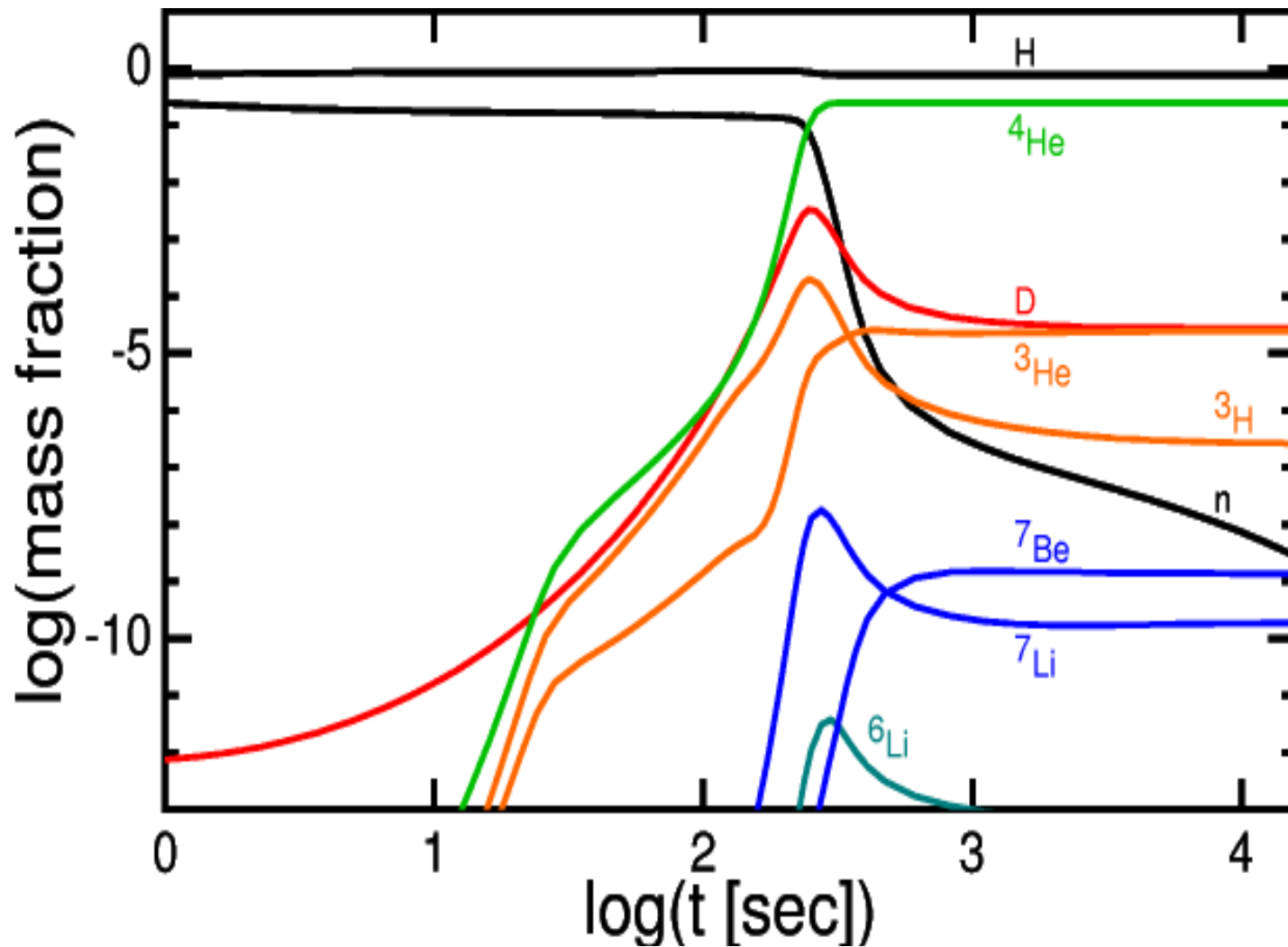


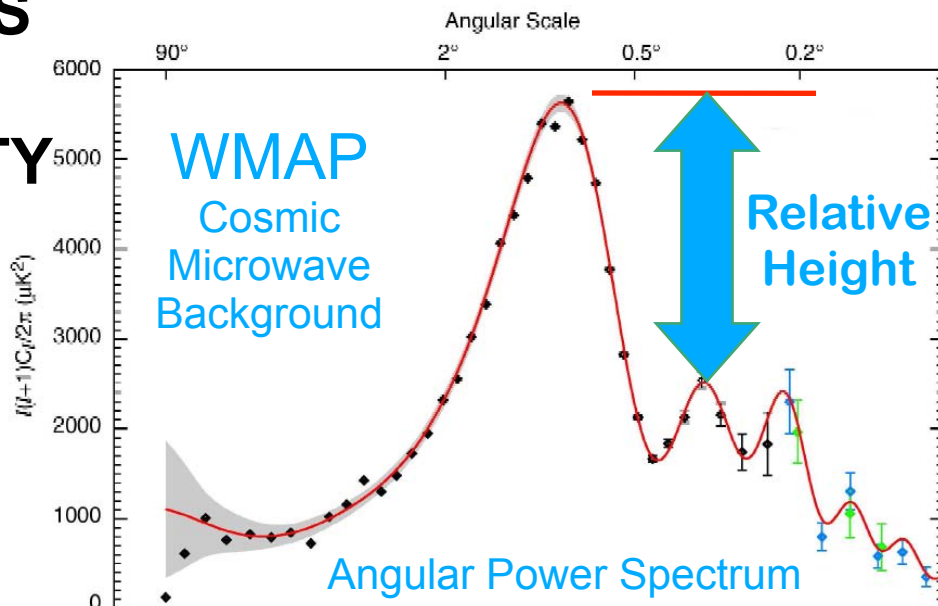
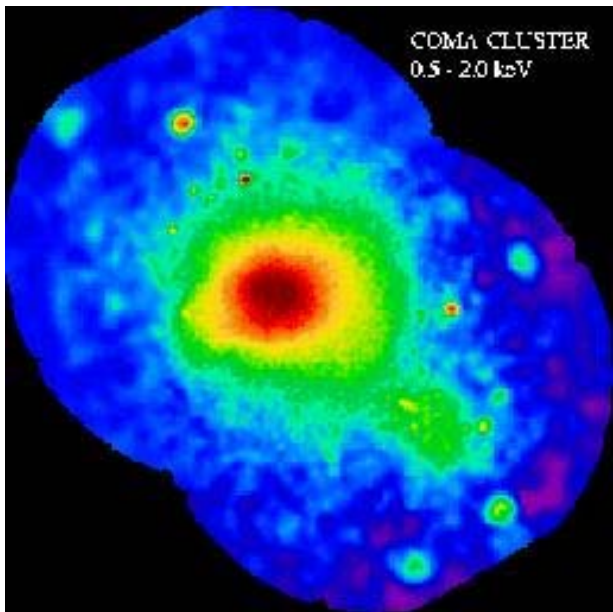
Figure 3.2. Evolution of light element abundances in the early universe. Heavy solid curves are results from Wagoner (1973) code; dashed curve is from integration of Eq. (3.27); light solid curve is twice the neutron equilibrium abundance. Note the good agreement of Eq. (3.27) and the exact result until the onset of neutron decay. Also note that the neutron abundance falls out of equilibrium at $T \sim \text{MeV}$.



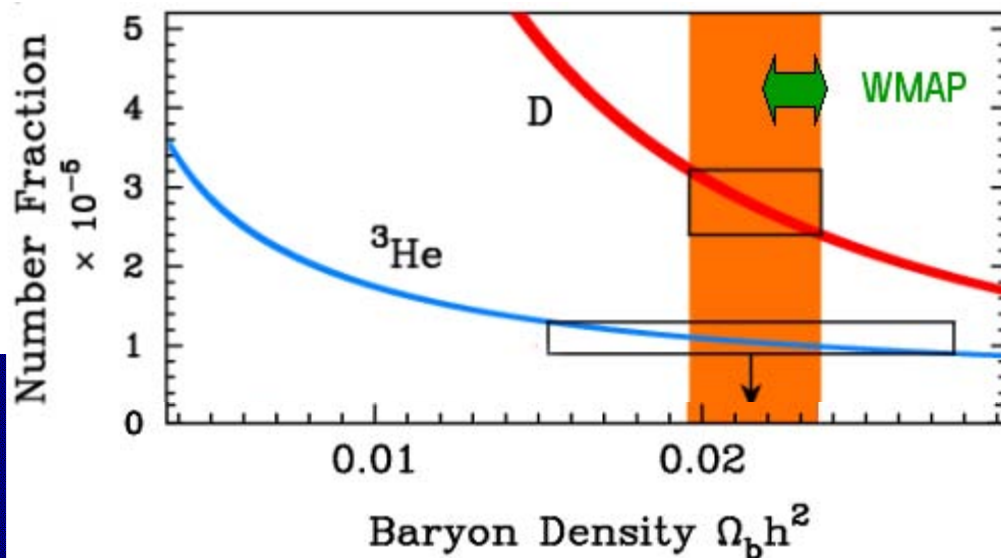
The detailed production of the lightest elements out of protons and neutrons during the first three minutes of the universe's history. The nuclear reactions occur rapidly when the temperature falls below a billion degrees Kelvin. Subsequently, the reactions are shut down, because of the rapidly falling temperature and density of matter in the expanding universe.

5 INDEPENDENT MEASURES AGREE: ATOMS ARE ONLY 4% OF THE COSMIC DENSITY

Galaxy Cluster in X-rays

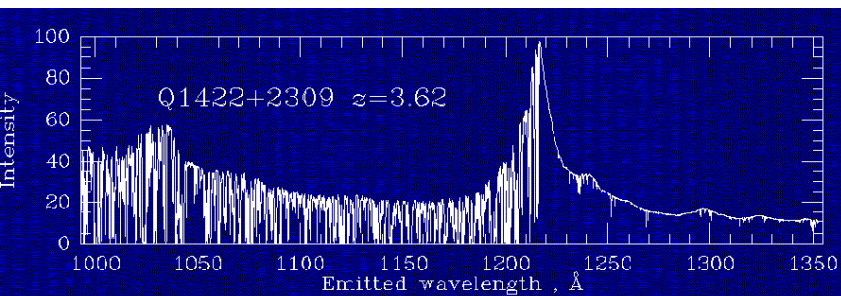


Deuterium Abundance
+ Big Bang Nucleosynthesis



& WIGGLES IN GALAXY P(k)

Absorption of Quasar Light

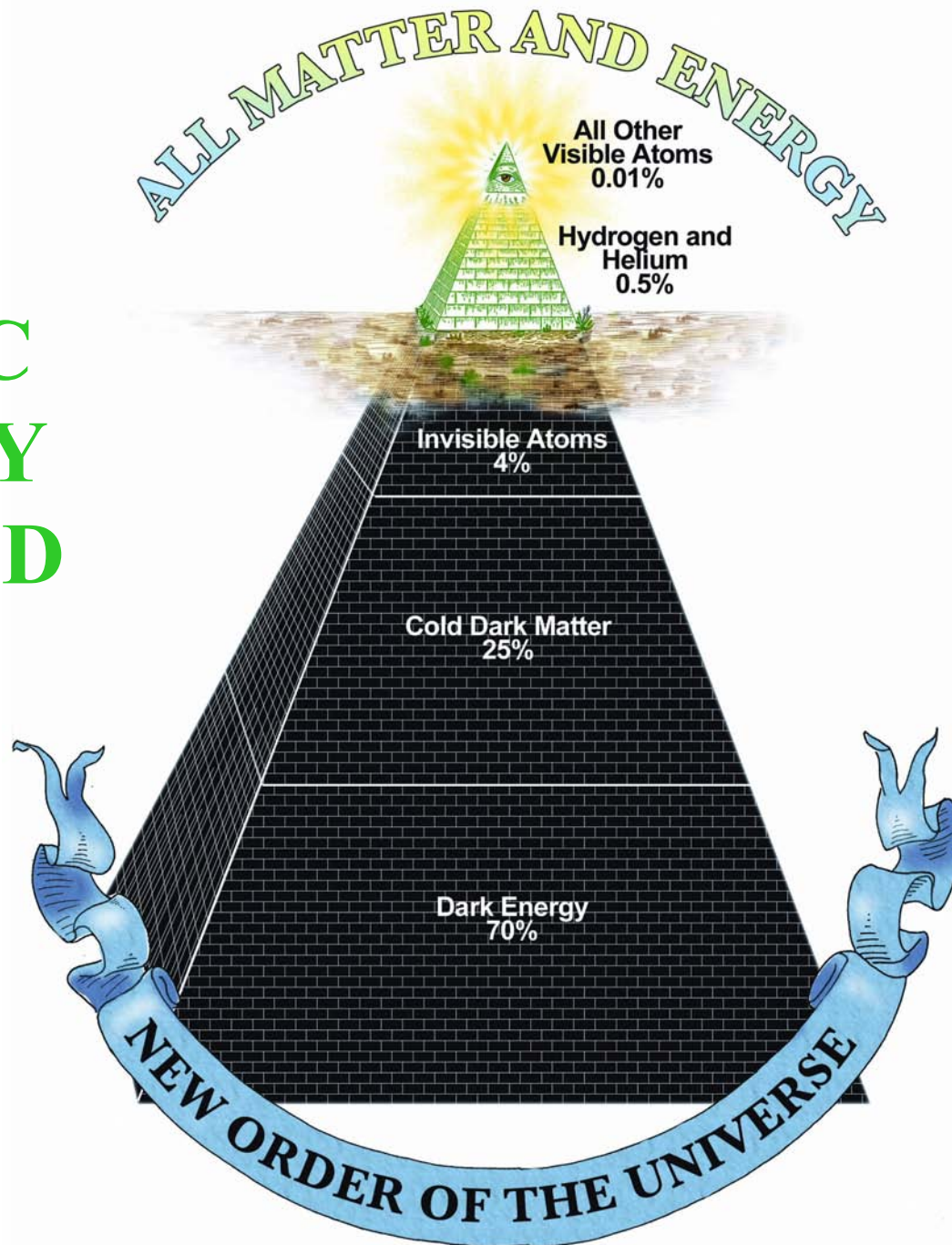




stardust

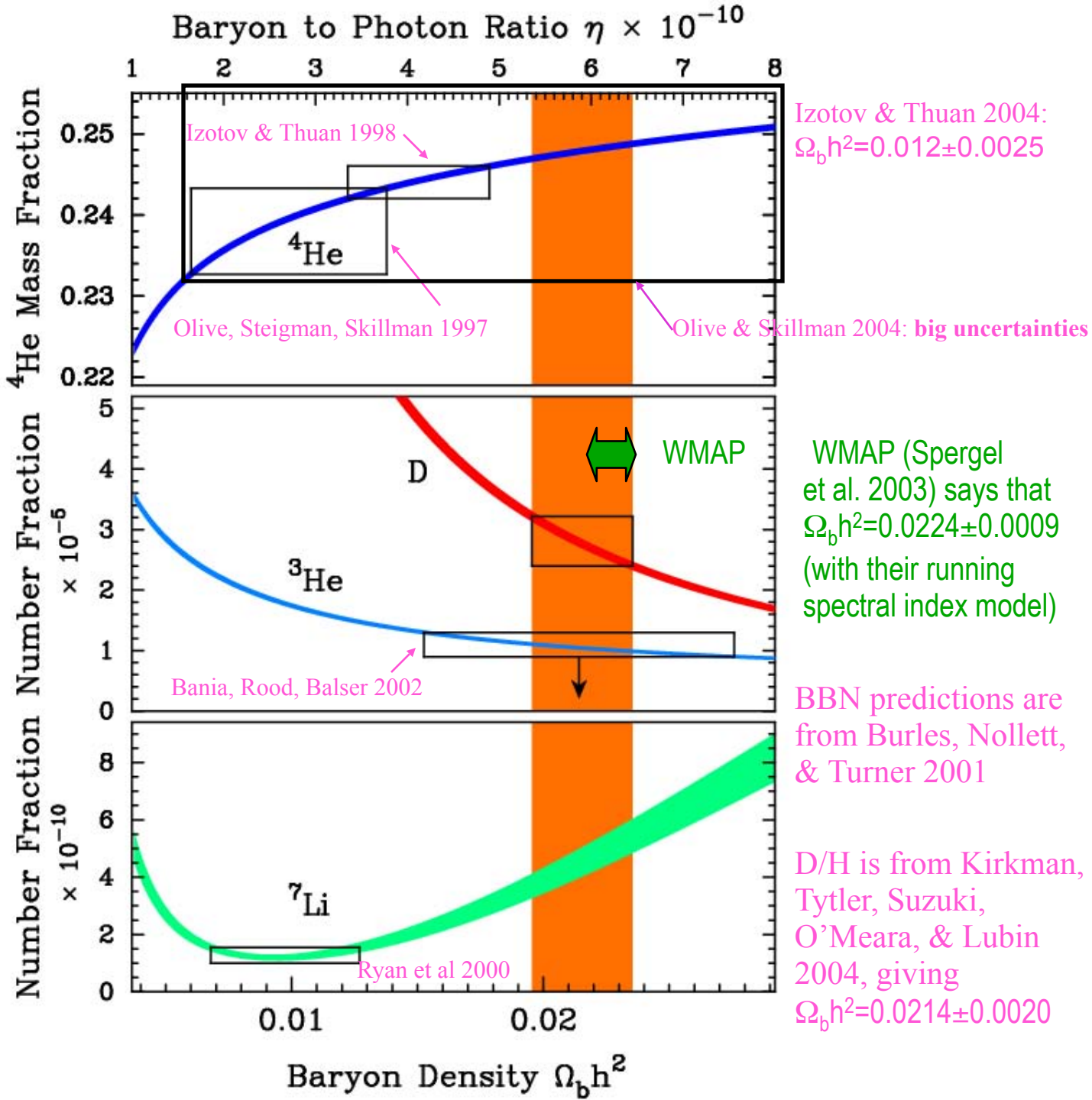
stars

COSMIC DENSITY PYRAMID

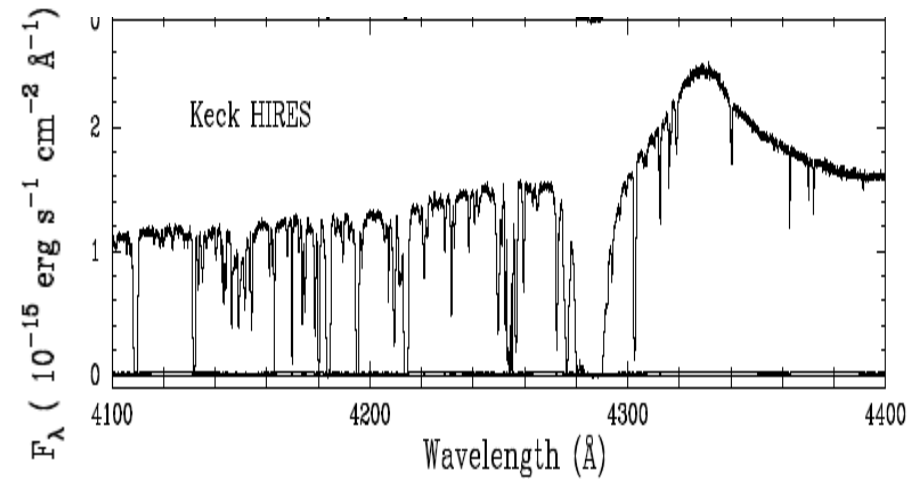


BBN
 Predicted
 vs.
 Measured
 Abundance
 s of D , ${}^3\text{He}$,
 ${}^4\text{He}$, and ${}^7\text{Li}$

${}^7\text{Li}$ IS NOW
 DISCORDANT



Deuterium absorption at redshift 2.525659 towards Q1243+3047



The Ly α absorption near 4285 \AA is from the system in which we measure D/H.

The detection of Deuterium and the modeling of this system seem convincing. This is just a portion of the evidence that the Tytler group presented in this paper. They have similarly convincing evidence for several other Lyman alpha clouds in quasar spectra.

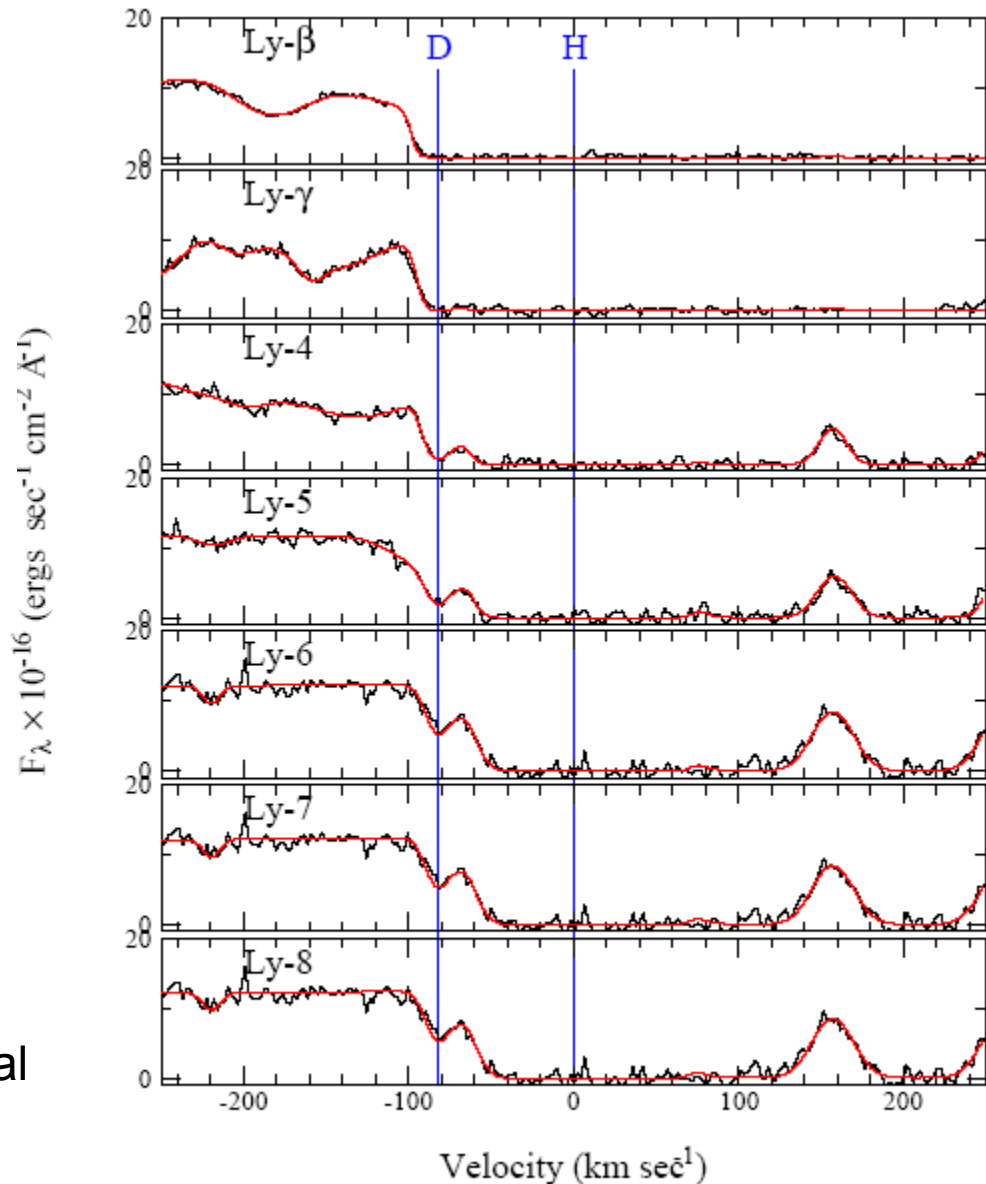
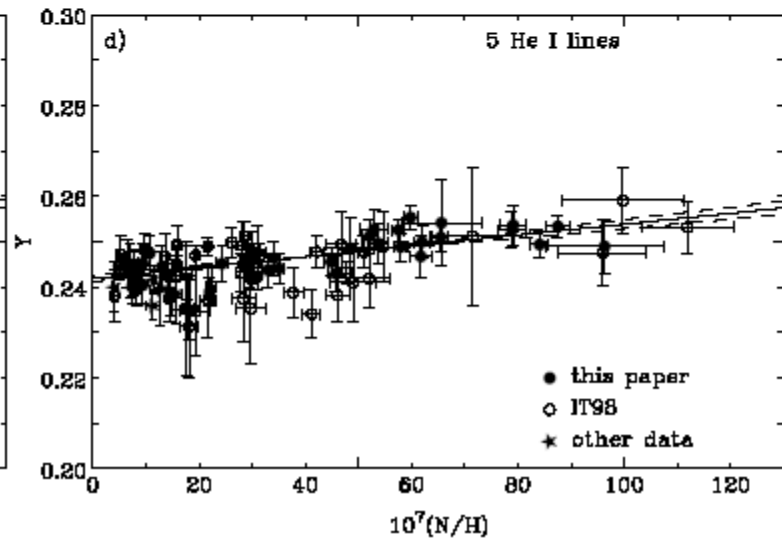
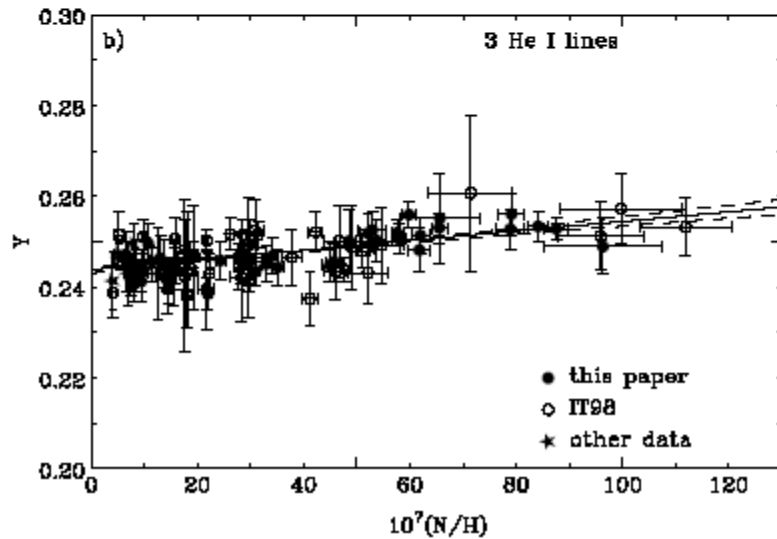
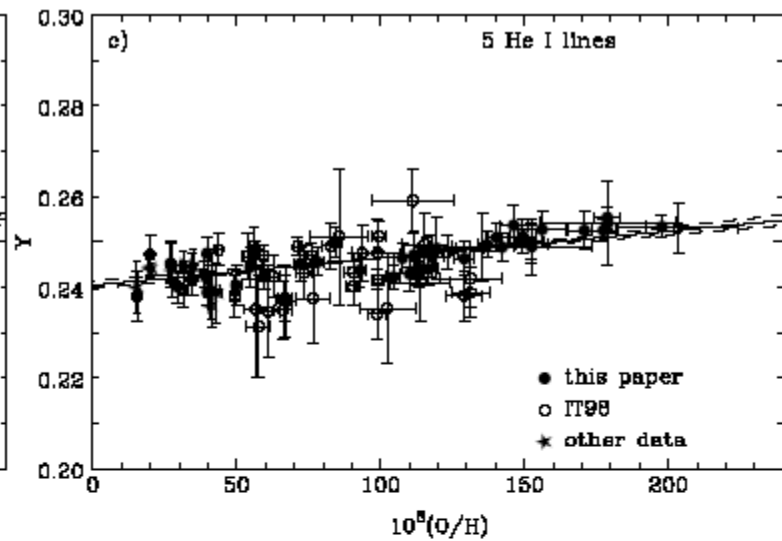
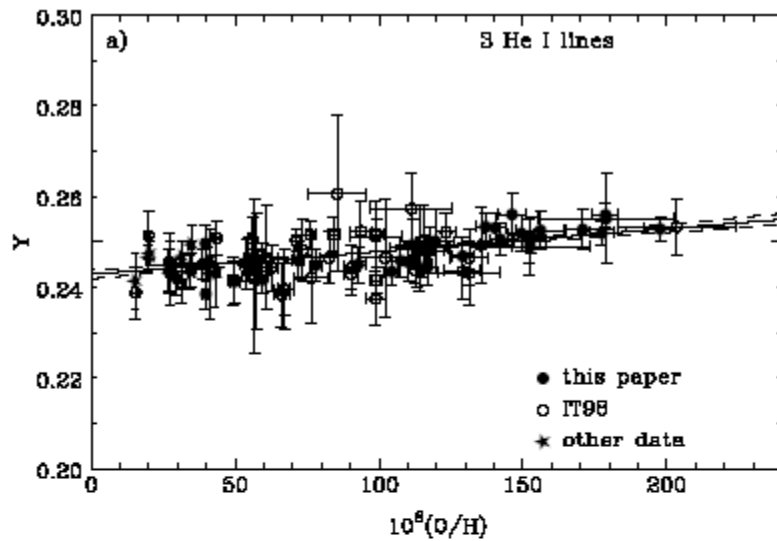


FIG. 7.— The HIRES spectrum of Ly-2 to 8, together with our model of the system, as given in Table 3.

Determination of primordial He^4 abundance Y_p by linear regression



$Y = M(^4\text{He})/M(\text{baryons})$, Primordial $Y \equiv Y_p = \text{zero intercept}$

Note: BBN plus $\text{D}/\text{H} \Rightarrow Y_p = 0.247 \pm 0.001$

The Li abundance disagreement with BBN may indicate new physics

Did Something Decay, Evaporate, or Annihilate during Big Bang Nucleosynthesis?

Karsten Jedamzik [Phys.Rev. D70 \(2004\) 063524](#)

*Laboratoire de Physique Mathématique et Théorique, C.N.R.S.,
Université de Montpellier II, 34095 Montpellier Cedex 5, France*

Results of a detailed examination of the cascade nucleosynthesis resulting from the putative hadronic decay, evaporation, or annihilation of a primordial relic during the Big Bang nucleosynthesis (BBN) era are presented. It is found that injection of energetic nucleons around cosmic time 10^3 sec may lead to an observationally favored reduction of the primordial ${}^7\text{Li}/\text{H}$ yield by a factor 2 – 3. Moreover, such sources also generically predict the production of the ${}^6\text{Li}$ isotope with magnitude close to the as yet unexplained high ${}^6\text{Li}$ abundances in low-metallicity stars. The simplest of these models operate at fractional contribution to the baryon density $\Omega_b h^2 \gtrsim 0.025$, slightly larger than that inferred from standard BBN. Though further study is required, such sources, as for example due to the decay of the next-to-lightest supersymmetric particle into GeV gravitinos or the decay of an unstable gravitino in the TeV range of abundance $\Omega_{\tilde{G}} h^2 \sim 5 \times 10^{-4}$ show promise to explain both the ${}^6\text{Li}$ and ${}^7\text{Li}$ abundances in low metallicity stars.

See also “Supergravity with a Gravitino LSP”
Jonathan L. Feng, Shufang Su, Fumihiro Takayama
[Phys.Rev. D70 \(2004\) 075019](#)

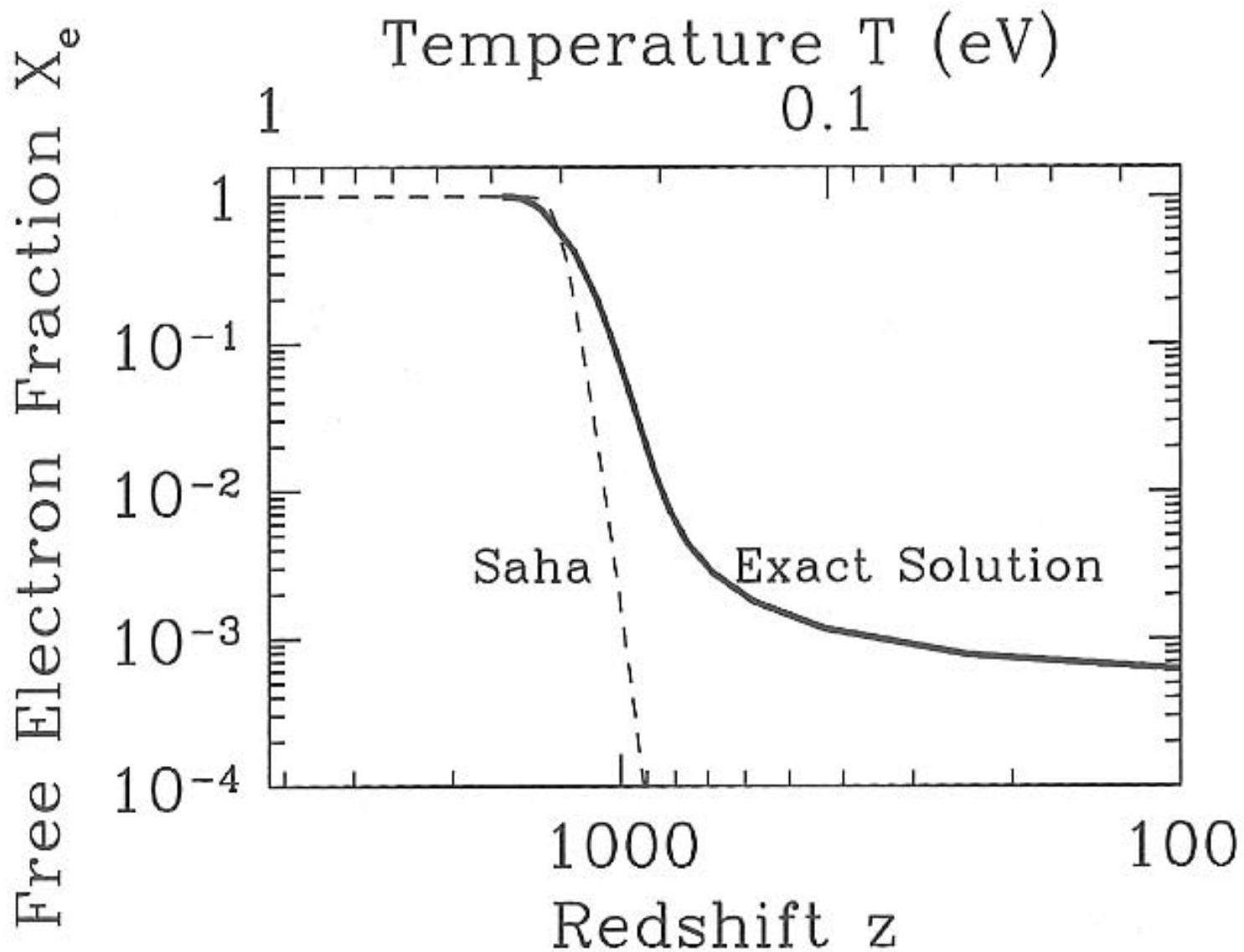


Figure 3.4. Free electron fraction as a function of redshift. Recombination takes place suddenly at $z \sim 1000$ corresponding to $T \sim 1/4$ eV. The Saha approximation, Eq. (3.37), holds in equilibrium and correctly identifies the redshift of recombination, but not the detailed evolution of X_e . Here $\Omega_b = 0.06$, $\Omega_m = 1$, $h = 0.5$.

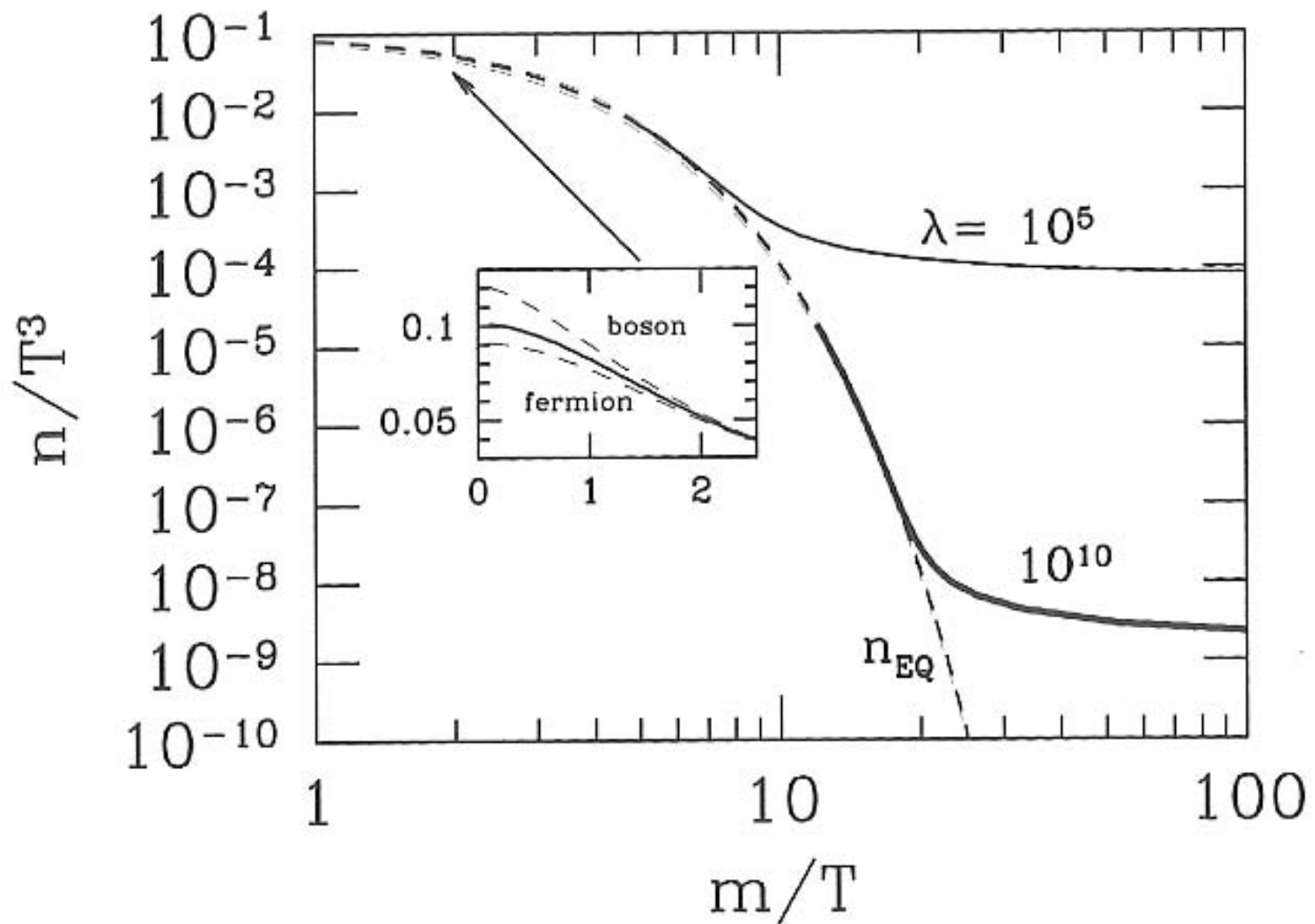


Figure 3.5. Abundance of heavy stable particle as the temperature drops beneath its mass. Dashed line is equilibrium abundance. Two different solid curves show heavy particle abundance for two different values of λ , the ratio of the annihilation rate to the Hubble rate. Inset shows that the difference between quantum statistics and Boltzmann statistics is important only at temperatures larger than the mass.